Article

Generation of SARS-CoV-2 escape mutations by monoclonal antibody therapy

Manon Ragonnet-Cronin [1,2,11] ✉, Rungtiwa Nutalai[3,11], Jiandong Huo[4,11] ✉, Aiste Dijokaite-Guraliuc [3,11], Raksha Das[3], Aekkachai Tuekprakhon[3], Piyada Supasa[3], Chang Liu[3,5], Muneeswaran Selvaraj[3], Natalie Groves [1], Hassan Hartman[1], Nicholas Ellaby[1], J. Mark Sutton[1], Mohammad W. Bahar[4], Daming Zhou [4,5], Elizabeth Fry [4], Jingshan Ren [4], Colin Brown [1], Paul Klenerman[6,7,8,9], Susanna J. Dunachie[6,7,9], Juthathip Mongkolsapaya[3,10], Susan Hopkins[1], Meera Chand[1], David I. Stuart [4] ✉, Gavin R. Screaton [3,11] ✉ & Sakib Rokadiya[1,11] ✉

COVID-19 patients at risk of severe disease may be treated with neutralising monoclonal antibodies (mAbs). To minimise virus escape from neutralisation these are administered as combinations e.g. casirivimab+imdevimab or, for antibodies targeting relatively conserved regions, individually e.g. sotrovimab. Unprecedented genomic surveillance of SARS-CoV-2 in the UK has enabled a genome-first approach to detect emerging drug resistance in Delta and Omicron cases treated with casirivimab+imdevimab and sotrovimab respectively. Mutations occur within the antibody epitopes and for casirivimab+imdevimab multiple mutations are present on contiguous raw reads, simultaneously affecting both components. Using surface plasmon resonance and pseudoviral neutralisation assays we demonstrate these mutations reduce or completely abrogate antibody affinity and neutralising activity, suggesting they are driven by immune evasion. In addition, we show that some mutations also reduce the neutralising activity of vaccine-induced serum.

Cases of SARS-CoV-2 infection were first reported in late-December 2019 in Wuhan[1], and the virus rapidly caused a global pandemic of coronavirus disease 2019 (COVID-19). As of June 2022, over half a billion cases have been reported, with more than six million deaths (https://covid19.who.int/). Being a positive-strand RNA virus, although its polymerase has some proofreading ability, SARS-CoV-2 has evolved rapidly with thousands of mutations identified already[2]. Certain

mutations can confer fitness advantages by increasing transmissibility or enabling evasion of humoral responses induced by natural infection or vaccination.

Since the outbreak started several variants of concern (VoC) (https://www.cdc.gov/coronavirus/2019-ncov/variants/variant-classifications.html) have emerged as dominant strains either globally[3–5] or regionally[6,7]. These variants contain multiple mutations

[1]Genomics Public Health Analysis, UK Health Security Agency, London, UK. [2]Centre for Global Infectious Disease Analysis, Imperial College London, London, England. [3]Wellcome Centre for Human Genetics, Nuffield Department of Medicine, University of Oxford, Oxford, UK. [4]Division of Structural Biology, Nuffield Department of Medicine, University of Oxford, The Wellcome Centre for Human Genetics, Oxford, UK. [5]Chinese Academy of Medical Science (CAMS) Oxford Institute (COI), University of Oxford, Oxford, UK. [6]Nuffield Department of Medicine, University of Oxford, Oxford, UK. [7]Oxford University Hospitals NHS Foundation Trust, Oxford, UK. [8]Translational Gastroenterology Unit, University of Oxford, Oxford, UK. [9]NIHR Oxford Biomedical Research Centre, University of Oxford, Oxford, UK. [10]Mahidol-Oxford Tropical Medicine Research Unit, Bangkok, Thailand, Department of Medicine, University of Oxford, Oxford, UK. [11]These authors contributed equally: Manon Ragonnet-Cronin, Rungtiwa Nutalai, Jiandong Huo, Aiste Dijokaite-Guraliuc, Gavin R. Screaton, Sakib Rokadiya. ✉e-mail: manonragonnet@uchicago.edu; dongdong.imm.ox.ac.uk@gmail.com; dave.stuart@strubi.ox.ac.uk; gavin.screaton@medsci.ox.ac.uk; sakib.rokadiya@nhs.net

mainly found in the gene encoding the viral spike, the major surface glycoprotein crucial for viral infection. The receptor-binding domain (RBD) of the spike, which initiates viral entry into the host cell by interacting with the host ACE2 receptor, is the major target for potent neutralising antibodies (mAbs). mAbs target the RBD in two different ways: most bind to a region on or in close proximity to the ACE2-binding surface of the RBD, whereby they prevent interaction of spike with ACE2 and hence block infection[8,9], others bind to non-ACE2 blocking sites on the RBD, and these mAbs may function to destabilise the trimeric spike[10–12].

Drug treatment can drive the evolution of pathogens, leading to rapid selection of advantageous mutations and emergence of resistant strains[13]. This process can result in failure of treatment; and the spread of resistance may cause new waves of infections. mAbs are usually prescribed in vulnerable populations where infections persist due to host immunosuppression, further increasing the likelihood of emergence of resistance (https://assets.publishing.service.gov.uk/government/uploads/system/uploads/attachment_data/file/1039516/S1430_NERVTAG_Antiviral_drug_resistance_and_use_of_Direct_Acting_Antiviral_Drugs_.pdf). There are potentially two ways to avoid mutational escape. Firstly, a cocktail of therapeutics may be developed to simultaneously bind different sites on the target, meaning that to escape, the pathogen will need to evolve two or more mutations, dramatically reducing the chances of escape. Drug cocktails are used to prevent the generation of escape mutations by a number of pathogens such as HIV[14] and TB[15]. REGEN-COV is a combination of two fully human non-competing mAbs, casirivimab (REGN10933) and imdevimab (REGN10987), both of which target the ACE2-binding interface of SARS-CoV-2 RBD and function to block RBD/ACE2 interaction[16]. In vitro experiments demonstrated that the combination could neutralise mutants selected[17] (https://www.covid19treatmentguidelines.nih.gov/therapies/anti-sars-cov-2-antibody-products/anti-sars-cov-2-monoclonal-antibodies/) using single components[18,19]. A previous report also suggested that treatment with REGEN-COV would be unlikely to lead to the emergence of escape mutants in both preclinical and human studies[20].

A second therapeutic strategy to prevent the accrual of escape mutations would be to develop therapeutics to target a highly conserved epitope that is mutationally constrained, i.e., a mutation of such an epitope would come at a high fitness cost to the pathogen, abrogating any selection advantage. Sotrovimab (VIR-7831/S309) binds in the region of the N-linked glycan at position 343 of the SARS-CoV-2 RBD; though not interfering with ACE2-binding, it is able to effectively neutralise the virus[21]. As this epitope is relatively well conserved among human and animal isolates of clade 1, 2 and 3 Sarbecoviruses (including SARS-CoV-1)[21], sotrovimab (developed from a mAb isolated from a SARS-CoV-1 infected case) was considered a broad neutraliser and perhaps able to resist mutational escape even as a monotherapy. However, the epitope is susceptible to mutation with Sotrovimab showing an approximately sixfold reduction in neutralisation of the Omicron variant[5].

In this work, we report the detection of viral mutations that are associated with drug resistance in patients treated with REGEN-COV (for infection with Delta variant) and sotrovimab (for infection with Omicron variants). We make use of the unprecedented genomic surveillance effort deployed for SARS-CoV-2 in the UK and develop a genomic approach for detecting emerging drug resistance (https://assets.publishing.service.gov.uk/government/uploads/system/uploads/attachment_data/file/1090992/11072022_SARS-CoV-2_Therapeutics_Technical_Briefing_4.pdf). We evaluate the binding behaviour of these viral mutants using surface plasmon resonance (SPR), and examine their impact on the neutralising activity of therapeutic antibodies using pseudoviral assays. Strikingly, the Delta variant is found to acquire mutations at two distinct sites targeted by casirivimab and imdevimab respectively, resulting in severe

impairment of neutralising activity of the cocktail. In addition, the Omicron BA.1 variant is found to gain single mutations at multiple sites which completely abolishes the binding and neutralisation activity of sotrovimab. Finally, the neutralisation titre of vaccine sera against these escape mutants is significantly reduced compared to the originating strain (i.e., Delta or BA.1 variants).

Results

Study population
The present analysis includes all patients who had received treatment in the UK, for whom at least one sample had been collected by 12 April 2022, for whom a viral genetic sequence was available and whose infection had been classified as Delta, BA.1 or BA.2. Our analysis comprised 17,284 sequences sampled fom 12,927 patients before treatment (Table 1, Sup Table 1). In the main analysis, sequences were considered post-treatment if patients were sampled at least 10 days after the day of treatment: 1627 sequences from 938 patients treated with one of casirivimab+imdevimab, molnupiravir, nirmatrelvir plus ritonavir (Paxlovid), remdesivir or sotrovimab.

Post-treatment mutation analysis
We compared amino-acid frequencies between pre- and post-treatment sequences. stratifying analyses by treatment, variant (Delta, BA.1 or BA.2), and gene. Nine amino acid residues displayed a significant ($p < 0.001$, one-sided Fisher's test) frequency change in post-treatment sequences compared to pre-treatment sequences, suggesting possible evidence of selection. All treatment-emergent substitutions were in the spike RBD region: E406D/Q, G446S/V, Y453F and L455F/S in patients infected with Delta and treated with casirivimab+imdevimab; P337R/S and E340A/D/K/V, K356T and R493Q in patients infected with BA.1 and treated with sotrovimab; and E340K in patients infected with BA.2 and treated with sotrovimab (Fig. 1). For molnupiravir, remdesivir and paxlovid, no significant ($p < 0.001$) mutations were observed in the available data.

Restricting the calculation to the three groups with identified associations: patients infected with Delta and treated with casirivimab+imdevimab and patients infected with BA.1 or BA.2 and treated with sotrovimab (Table 1), a total of 86 post-treatment (≥10 day) sequences from 59/240 (24.59%) patients had at least one of the identified mutations, compared to 15 sequences from 14/6116 (0.20%) pre-treatment patients (Table 2; $p < 10^{-16}$, one-sided Fisher's test). Of 1557 patients infected with Delta and treated with casirivimab+imdevimab, 11 (0.70%) developed a mutation after 10 days, compared to 46/3221 (1.43%) patients infected with BA.1 and treated with sotrovimab and 2/1338 (0.15%) patients infected with BA.2 and treated with sotrovimab, suggesting comparable escape rates for the two mAbs. Eleven post-treatment patients had >1 mutation: three patients infected with Delta treated with casirivimab+imdevimab had a combination of G446V and L455F, one had G446S and L455S and one had G446V and Y453F. We examined the raw reads and confirmed that for all these patients, both mutations were present on most contiguous raw reads. Among BA.1 patients treated with sotrovimab, four had a combination of E340A and R493Q, one had E340D and R493Q and one had K356T and R493Q.

The analysis was repeated with a different threshold for post-treatment sequences: at least one or five days after treatment. While datasets were much larger when a shorter interval was considered, the strength of the signal became stronger as the interval was lengthened, lending support to the validity of our findings (Figure S1).

Within our dataset, we searched for patients with sequences sampled before and after treatment. We found 25 patients with Delta infections and matched sequences of whom seven switched from the wild-type amino acid to one of the treatment-emergent substitutions identified (Table 2), Among 49 BA.1 patients with matched sequences, 19 had a treatment-emergent substitution. The single BA.2 patient with

Table 1 | Data set sizes (number of patients)

Treatment	Variant	Number of patients (pre-treatment)	Number of patients (≥1 day post-treatment)	Number of patients (≥5 day post-treatment)	Number of patients (≥10 day post-treatment)	Number of patients (≥14 day post-treatment)
Casirivimab and imdevimab	BA.1	137	85	73	64	58
Casirivimab and imdevimab	BA.2	0	11	12	12	12
Casirivimab and imdevimab	Delta	1557	227	123	67	50
Molnupiravir	BA.1	1411	150	104	67	41
Molnupiravir	BA.2	228	17	11	8	5
Molnupiravir	Delta	24	7	6	4	1
Paxlovid	BA.1	276	18	8	6	2
Paxlovid	BA.2	598	40	15	10	5
Paxlovid	Delta	0	1	1	1	1
Remdesivir	BA.1	872	397	305	258	227
Remdesivir	BA.2	187	92	76	65	65
Remdesivir	Delta	3054	703	334	201	133
Sotrovimab	BA.1	3221	380	240	148	114
Sotrovimab	BA.2	1338	112	50	25	18
Sotrovimab	Delta	24	5	5	2	2

a pre- and post-treatment sequence had mutated from E to K at position 340.

Finally, we evaluated how often the treatment-emergent mutations occurred in groups treated with a different drug. In BA.1/BA.2 patients who were never treated with sotrovimab ($n = 985$), 0.25% had the R493Q mutation. In Delta patients who were never treated with casirivimab and imdevimab ($n = 1555$), 0.34% had the G446V mutations. None of the other mutations were found in these groups, indicating that all the treatment-emergent mutations were highly specific to the corresponding drug.

Frequency of mutations in UK genomic database

For each mutation identified, we ascertained its frequency in the UK genomic database from September 2022 onwards. The frequency of the mutations listed previously within the UK genomic data set for mutations associated with casirivimab and imdevimab in Delta sequences ($n = 763,511$) were: 6 E406D; 7 E406Q; 163 G446S; 1946 G446V; 12 Y453F; 179 L455F; 1 L455S. The frequency of mutations post-sotrovimab treatment with the BA.1 variant ($n = 742,992$) was: 11 P337R; 32 P337S; 39 E340A; 82 E340D; 52 E340K; 5 E340V; 57 K356T; 1214 R493Q. The frequency of mutations post-sotrovimab treatment with the BA.2 variant ($n = 407,161$) was: 10 E340K. While above, a total of 86/719 (12.1%) post-treatment (≥1 day) patients had at least one of the identified mutations; the frequency of any mutation in the variants of interest in the genomic surveillance dataset was only 3653/1,862,686 (0.20%, identical to the frequency in the pre-treatment dataset; $p < 10^{-16}$, one-sided Fisher's test).

Overall, these data demonstrate a significant enrichment of mutations in the post-treatment sequences compared to the pre-treatment group and compared to the genomic database as a whole, strongly implicating them as mutations selected for escape from mAb therapy.

Mapping of mutations to the spike

Figure 2 shows the positions of the mutations found to be of high significance. All mutations occur in the RBD of the SARS-CoV-2 spike.

In Fig. 2a the mutations associated with sotrovimab treatment are mapped to the structure of the Omicron BA.1 RBD and sotrovimab complex (7TLY [https://www.rcsb.org/structure/7TLY])[22]. Note that
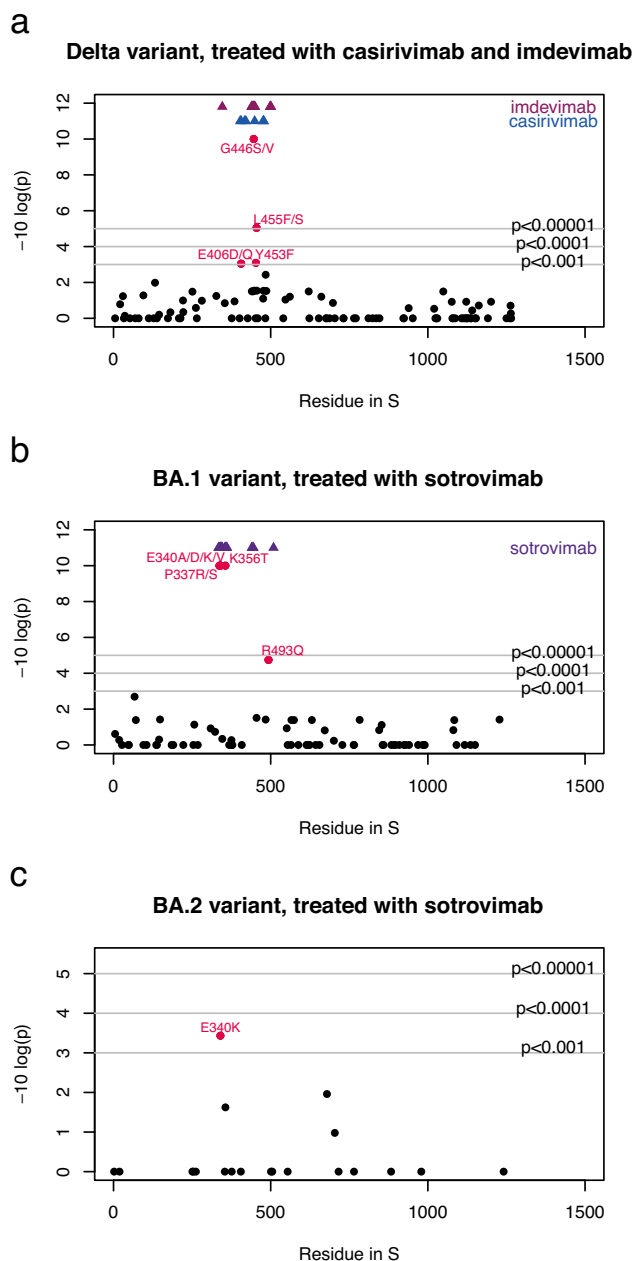
RBD residues 337, 340, and 356 cluster tightly forming an interaction hotspot with the antibody heavy chain CDR3 in particular (Fig. 2b). W105 and F106 of the CDR3 form a key 4-layer hydrophobic sandwich with residues 337 and 356 of the RBD (W105:P337:F106:K356), whilst E340 pins down the CDR3 loop by a remarkable set of interactions with the amide nitrogens of residues 104-106, which are arranged rather as an open helix capped with exquisite specificity by E340. This suggests that the observed mutations P337R/S; E340A/D/K/V; K356T will all disrupt this binding hotspot. In contrast Q493R is distal to the epitope, on the edge of the ACE2 footprint (Fig. 2a), so there is no obvious reason for this mutation to affect antibody binding.

The mutations associated with casirivimab and imdevimab treatments are shown in Fig. 2c, mapped to the structure of the Delta RBD containing the L452R mutation (7ORB [https://www.rcsb.org/structure/7ORB])[19], where the binding of casirivimab and imdevimab is inferred from the reported structure of the complex with early pandemic RBD (6XDG [https://www.rcsb.org/structure/6XDG]), the RMSD in Cα positions between early pandemic and Omicron BA.1 RBDs is 1.16 Å and we are confident that this inference is secure). The mutations observed fall into two areas on the surface of the RBD. Positions 406, 453 and 455 are clustered together at the back of the neck region[8] lying under the CDR1 of the casirivimab heavy chain and forming a nest of interactions (Fig. 2d). These mutations would be expected to affect binding of this antibody. In contrast G446 rests tightly against N57 and Y59 of the light chain CDR2 of imdevimab (Fig. 2e) and any change to a larger side chain such as the G446S/V mutations observed, would be expected to abrogate binding.

Experimental measurement of escape by mutants identified from patients treated with REGEN-COV

We constructed a panel of pseudotyped lentiviruses[23] expressing the spike from the identified escape mutants (Fig. 3). Pseudoviral neutralisation assays showed that activity of imdevimab against the Delta +G446V mutant was completely knocked out, whilst casirivimab showed >10-fold reductions in the neutralisation titre of Delta+Y453F (16-fold), Delta+L455F (17-fold) and Delta+L455S (155-fold), compared to the wild-type Delta variant (Fig. 3A, C)

As casirivimab remained fully active against the Delta+G446V mutant, and imdevimab was still able to potently neutralise the Delta

a

Delta variant, treated with casirivimab and imdevimab

b

BA.1 variant, treated with sotrovimab

c

BA.2 variant, treated with sotrovimab

Fig. 1 | *P* values for differences in spike amino-acid frequencies between pre- and post-treatment sequences. a Patients infected with Delta and treated with casirivimab/imdevimab ($n = 1557$ pre-treatment and $n = 67$ post-treatment), **b** patients infected with BA.1 and treated with sotrovimab ($n = 3221$ pre-treatment and $n = 148$ post-treatment), and **c** patients infected with BA.2 and treated with sotrovimab ($n = 1338$ pre-treatment and $n = 25$ post-treatment). Amino acid frequencies were compared between pre-and post-treatment samples (at least 10 days after treatment) at each site in the spike sequence alignment. *P* values for each site were calculated using a one-sided Fisher's test, and *p* values were log-transformed and inversed for visualisation so that sites with diverging values appear higher up on the figure. Only sites with some variability (>1 amino acid) are shown. The horizontal lines indicate *p* value thresholds of $p < 0.001$, $p < 0.0001$ etc. Residues with diverging frequencies ($p < 0.001$) are highlighted in red, with the observed amino acid change indicated in text. Residues known to interact with each drug are indicated in blue and purple at the top of the figure. Nine sites are highlighted in red in the figure: E406D/Q ($p = 9 \times 10^{-4}$), G446S/V ($p < 10^{-16}$), Y453F ($p = 0.000809$) and L455F/S ($p = 9 \times 10^{-6}$) in patients infected with Delta and treated with casirivimab +imdevimab; P337R/S ($p < 10^{-16}$) and E340A/D/K/V ($p < 10^{-16}$), K356T ($p < 10^{-16}$) and R493Q ($p = 1.8 \times 10^{-5}$) in patients infected with BA.1 and treated with sotrovimab; and E340K ($p = 0.000369$) in patients infected with BA.2 and treated with sotrovimab. See also Figure S1. No adjustments were made for multiple comparisons.

+Y453F and Delta+L455F/S mutants, the combination of casirivimab and imdevimab retained neutralisation potency against all these single mutants. However, the combined mutations of Delta+G446V + Y453F and Delta+G446V + L455F not only led to complete knock-out of the neutralising activity of imdevimab, but also severe knock-down of casirivimab activity. As a result, the neutralisation titre of casirivimab +imdevimab was reduced 1097-fold against Delta+G446V + Y453F and 318-fold against the Delta+G446V + L455F. This is consistent with the finding of these pairs of mutations occurring together on single Delta RBD sequences described above.

To confirm that the observed effects on neutralisation were directly attributable to the change in RBD/mAb interaction, we measured the affinity of mAbs and RBD mutants by surface plasmon resonance (SPR) (Figs. S2, S3, Table 3A). This analysis also showed that the G446V mutation almost abolished the binding of imdevimab, and in the meantime caused a modest reduction (1.8-fold) in the binding affinity of casirivimab (Table 3A). The L455S, E406D and E406Q single mutations mainly affect casirivimab. SPR analysis showed a 369-fold, 20-fold and 38-fold decrease in the affinity of casirivimab for Delta +L455S, Delta+E406D and Delta+E406Q respectively. The neutralisation titre of casirivimab was reduced 65-fold, 2-fold and 12-fold against these three mutants respectively (Fig. 3C, Table 3A). However, since imdevimab was unaffected, the casirivimab+imdevimab combination retained potent neutralising activity against these mutants.

Interestingly, an additive effect on reducing casirivimab binding was seen for the combination of mutations resulting in an overall 347-fold and decrease in affinity for G446V + Y453F and 192-fold decrease for G446V + L455F. As expected, binding of imdevimab to Delta +G446V + Y453F and Delta+G446V + L455F was almost completely impaired. Overall, the acquisition of double mutations has rendered substantial loss in sensitivity to the REGEN-COV regime.

Experimental measurement of escape by mutants identified from patients treated with sotrovimab

BA.1 mutations P337R/S and E340A/D/K/V, led to complete knock out of neutralisation by sotrovimab (Fig. 3B, D). Although the BA.1 + R493Q (reversion to Wuhan wild type) was also identified as a post-treatment-emergent mutation, no obvious effect on the neutralising activity of sotrovimab was observed. The RBDs of BA.1 + P337R/S and BA.1 + E340A/D/K/V were successfully expressed to allow examination of their binding with sotrovimab (Figure S3). The affinity of sotrovimab was reduced by 1951-fold to 20241-fold compared to the wild-type BA.1 RBD, explaining why these mutants were resistant to sotrovimab neutralisation (Table 3D).

Neutralisation of escape mutants by vaccine serum

Neutralisation assays were performed using serum obtained 28 days following a third dose of Pfizer-BioNtech vaccine BNT162b2[24] (Fig. 4). Following 3 doses of BNT162B a 1.9-fold and 1.5-fold decrease was observed for Delta+G446V + Y453F and Delta+G446V + L455F respectively, compared to wild-type Delta ($p < 0.0001$); whilst a 2-fold, 1.2-fold and 3.8-fold reduction was seen for BA.1 + P337S, BA.1 + E340K and BA.1 + K356T respectively compared to wild-type BA.1 ($p < 0.0001$, $p = 0.0082$ and $p < 0.0001$).

Discussion

Individuals infected with the currently dominant SARS-CoV-2 Omicron variant have been shown to have a lower likelihood of severe disease and hospitalisation compared with previous variants. However, many people still suffer from severe disease[25] and this proportion could be higher in populations with lower levels of infection- or vaccine-induced immunity.

Although the current mortality rates are much lower than in 2020 (https://www.ons.gov.uk/peoplepopulationandcommunity/healthandsocialcare/conditionsanddiseases/articles/coronaviruscovid

Table 2 | Frequency of each mutation

Variant	Treatment	Gene	Mutation	Frequency in pre-treatment patients	Frequency in treated patients	p value	Switches
Delta	Casirivimab and imdevimab	spike	E406D/Q	0 (0%)	1 (1.2%)	9×10^{-4}	1/35
Delta	Casirivimab and imdevimab	spike	G446S/V	2 (0.1%)	8 (9.8%)	$p < 10^{-16}$	4/35
Delta	Casirivimab and imdevimab	spike	Y453F	0 (0%)	2 (2.4%)	0.000809	0/35
Delta	Casirivimab and imdevimab	spike	L455F/S	2 (0.1%)	4 (4.9%)	9×10^{-6}	2/35
BA.1	sotrovimab	spike	P337R/S	0 (0%)	12 (5.7%)	$p < 10^{-16}$	3/49
BA.1	sotrovimab	spike	E340A/D/K/V	4 (0.1%)	31 (14.7%)	$p < 10^{-16}$	11/49
BA.1	sotrovimab	spike	K356T	0 (0%)	5 (2.4%)	$p < 10^{-16}$	4/49
BA.1	sotrovimab	spike	R493Q	1 (0.03%)	4 (1.9%)	1.8×10^{-5}	1/49
BA.2	sotrovimab	spike	E340K	1 (0.05%)	2 (8%)	0.000369	1/1

p values were calculated using a one-sided Fisher's test. No adjustments were made for multiple comparisons.

19latestinsights/deaths), as of June 2022 over 300 people died from COVID-19 every week within the UK (https://coronavirus.data.gov.uk/details/deaths). Individuals who are unable to mount an adequate immune response from vaccination or for whom vaccination is not recommended are at particular risk. It is this vulnerable population, who tend to suffer from chronic COVID-19 infections, who are targeted to receive mAb therapies either therapeutically or prophylactically. In the UK, the highest-risk clinical subgroups who are immunosuppressed are eligible for these therapies (https://www.gov.uk/government/publications/higher-risk-patients-eligible-for-covid-19-treatments-independent-advisory-group-report/defining-the-highest-risk-clinical-subgroups-upon-community-infection-with-sars-cov-2-when-considering-the-use-of-neutralising-monoclonal-antibodies).

While commercial anti-SARS-CoV-2 therapeutic mAbs have been shown to be effective treatments for COVID-19[26,27], various studies have reported severe reductions or complete knock-out of their neutralising activities against Omicron variants[5,22,28,29]. As sotrovimab was shown to be unable to effectively neutralise Omicron BA.2, in April 2022 the FDA announced that sotrovimab was no longer authorised to treat COVID-19 as BA.2 became the dominant variant (https://www.fda.gov/drugs/drug-safety-and-availability/fda-updates-sotrovimab-emergency-use-authorization) and in the UK, sotrovimab is no longer widely used.

In a recent study, the Delta variant was reported to develop P337L/T and E340K/A/V resistance mutations in patients treated with sotrovimab[30]. Here we report the identification of BA.1 escape mutations in patients who received sotrovimab treatment. In addition to mutations occurring at the P337 and E340 residues, we also identify a novel K356T mutation. These mutations abolish the binding and hence neutralising activity of sotrovimab. Q493R is also found, a reversion to the sequence found in early pandemic viruses and in BA.4/5. This mutation is distal to the sotrovimab footprint, has no effect on antibody binding but has been reported to increase the affinity for ACE2 (Wang et al., 2022), suggesting improved receptor binding rather than escape from antibody binding may be the driver for selection. These observations suggest that monotherapy is likely to be impacted by emerging variants and induce treatment-emergent resistance, even if the drug targets an epitope that is relatively conserved among Sarbecoviruses.

In contrast to the single agent sotrovimab, the REGEN-COV regime, containing a combination of two mAbs that target non-overlapping epitopes, would be expected to be more resistant to mutational escape. Indeed, previous studies have shown that REGEN-COV was able to effectively prevent emergence of escape mutants not only in vitro, but also in in vivo animal and human studies[18,20]. However, in our detailed study, we observe that treatment with the dual agent REGEN-COV led, in some individuals, to the Delta variant acquiring pairs of mutations that simultaneously impair the binding of both components of REGEN-COV, leading to up to 1000-fold reduction in

neutralisation titres. All the mutations we identified had been predicted in a mapping exercise where the impact of every potential mutation in the spike protein was tested. The study revealed that pseudoviruses with an E406W mutation were able to escape from both REGEN-COV compounds[31]. This mutation did not occur in our small dataset. Two nucleotide changes are required for this change in amino acid; however, single nucleotide changes at the site were identified and found to be significant.

It is uncertain how the virus was able to gain the combined resistance mutations during therapy, however, accelerated viral evolution has been documented in immunocompromised patients who could suffer from persistent SARS-CoV-2 infections for many months, with mutations found predominantly in the RBD and other regions of the spike[32]. One possibility is that viruses harbouring mutations resistant to one component of REGEN-COV might have already emerged in such patients prior to the cocktail treatment, and the medication then drove selection of a second mutation, leading to an overall impairment of the therapy, perhaps accelerated by viral recombination. If accelerated virus evolution has facilitated escape via a bystander effect (for instance mutations driven by modulation of receptor binding) this might be an additional argument for attempting to find neutralising antibodies that bind in more conserved regions, although we find that increased receptor affinity is selected in some BA.1 infected patients treated with sotrovimab, which binds a relatively conserved epitope. However, viruses bearing single escape mutations were identified in patients under the REGEN-COV treatment. In effective combination therapy, these mutants would be neutralised by one of the components. This raises the question of whether the concentration of the mAbs might be unable to reach the desired level in vivo, for example due to limited or differential bioavailability in certain parts of the body, creating a favourable environment for viruses to develop resistance. Patient samples were not available to test pre-treatment endogenous neutralisation.

The simplest way to mitigate escape is probably to use a more complex cocktail of non-competing mAbs, indeed it has been shown that such a combination was able to retain antiviral potency through up to eleven consecutive serial passages[20]. Combining mAbs with antivirals is another option, or devising clinical approaches based on patient profile together with using the correct dose for bioavailability. It could also be important to perform genotyping for variants prior to administration of mAb therapy, particularly in chronically infected immunocompromised cases[33]. However, patients prescribed treatment for COVID-19 infections are usually started on therapy the same day, and so the turnaround time between sampling and sequence analysis would have to be substantially shortened for clinical use.

Finally, it is concerning that the neutralisation titre of vaccine serum was reduced against escape mutants evolved from both treatment regimes in two different virus variants. This is not altogether surprising, as the mAbs chosen for therapeutic use target important
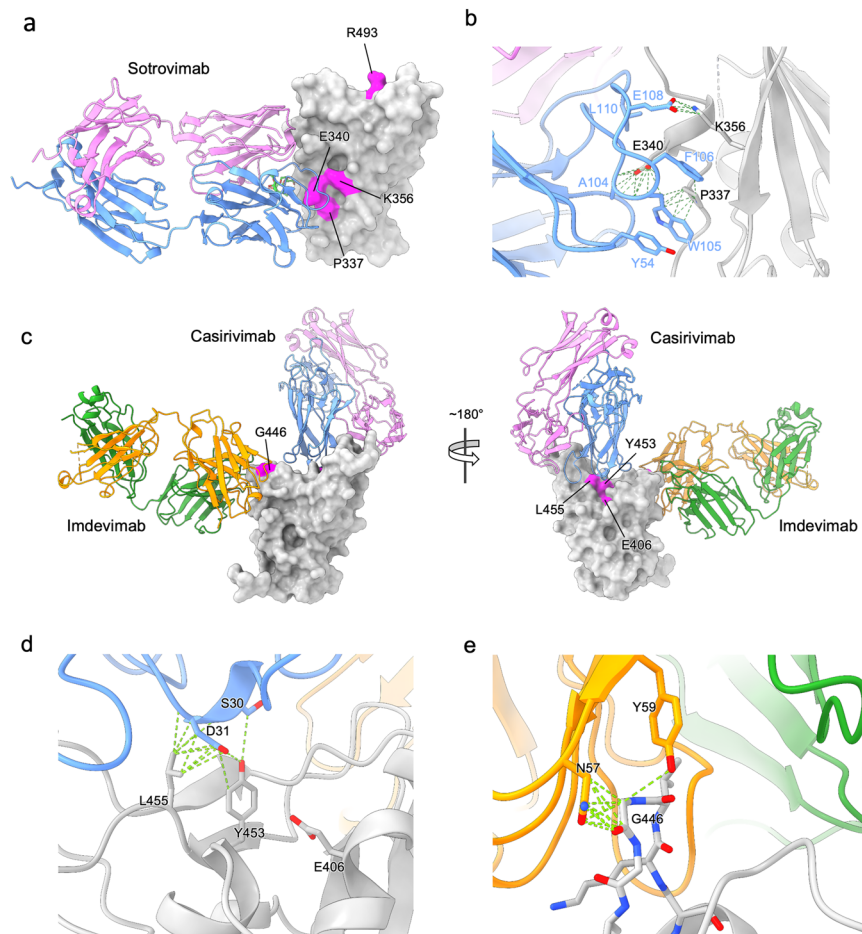
Fig. 2 | Structural modelling of mutations mapped to the spike RBD. a Model of the Omicron RBD (7TLY) docked with S309 (sotrovimab). Omicron RBD is shown as a grey surface from an approximate front view, S309 as cartoon ribbons with heavy and light chains coloured separately. Mutation sites mapped to the RBD surface are coloured magenta and labelled. **b** Close-up view of the interface between the P337, E340, K356 patch of residues with the S309 heavy chain. Potential hydrogen bonds and hydrophobic interactions are shown as green dashed lines. **c** Model of the Delta RBD docked with REGEN-COV mAbs casirivimab and imdevimab shown from approximate front (left) and back (right) views. Delta RBD is shown as a grey surface and mutation sites E406, G446, Y453 and L455 are coloured magenta and labelled. **d** Close-up view of the interface between E406, Y453 and L455 with casirivimab. **e** Close-up view of the interface between G446 with imdevimab. Potential hydrogen bonds and hydrophobic interactions are shown as green dashed lines.

neutralising epitopes on the SARS-CoV-2 RBD. Whether mAb therapy can drive the generation of novel highly transmissible variants is not clear; our study using in vitro neutralisation gives no indication how fit these variants would be in the general population. It also seems unlikely that mAb-driven escape in the extremely small number of patients given therapy will markedly accelerate generation of novel variants compared to what is happening in the pandemic at large, with millions of infections occurring every day, in an increasingly naturally exposed or vaccinated population, where the selection pressure for antibody escape is already extreme. Indeed, most selection pressure is not driven by antibody pressure and occurs in untreated individuals as the virus evolves during successive transmissions, but this process can also lead to the loss of the therapeutics potential of antibodies. Nonetheless, the repeated and perhaps inconsistent use of mAb therapy in chronically infected individuals, who have been documented to harbour virus for months and in some cases more than a year, should be closely monitored, an emphasis should be placed on treatment adherence. The potential for the virus mutating should not discourage us from deploying clinical interventions such as vaccines and treatment, as interventions prevent severe infections and reduce overall case numbers – making the emergence of a novel variant less likely. The analysis of post-treatment sequence datasets and potential transmission of post-treatment-emergent mutations is performed

regularly by the UK Health Security Agency and published online (https://www.gov.uk/government/publications/covid-19-therapeutic-agents-technical-briefings) to rapidly detect treatment-emergent mutations and react if necessary.

Although our results are compelling, our study suffers from several limitations. We used in vitro neutralisation assays and may underestimate the neutralisation potential of mAb in vivo, where the effects of antibody-dependent cell-mediated cytotoxicity and complement may increase activity. In addition, using in vitro systems we are unable to determine whether the escape mutations selected by mAb therapy would be fit to compete with natural viral variants in natural infections. We did not look at deep sequence data to look at changes in frequencies of minor variants over time, our sequences are consensus reads. Our single amino acid approach may miss compensatory mutations that do not come out as significant in a large-scale analysis but may be important within patients who have already developed one treatment-emergent substitution. Future research should examine the within-patient population dynamics of viral mutations and use longitudinal analyses to identify low-frequency variants and estimate the strength of selection. Linkage to clinical data such as duration of infection and chronic immune deficiencies will help identify the predictors of resistance. Viral loads and clinical data were not available to us. This
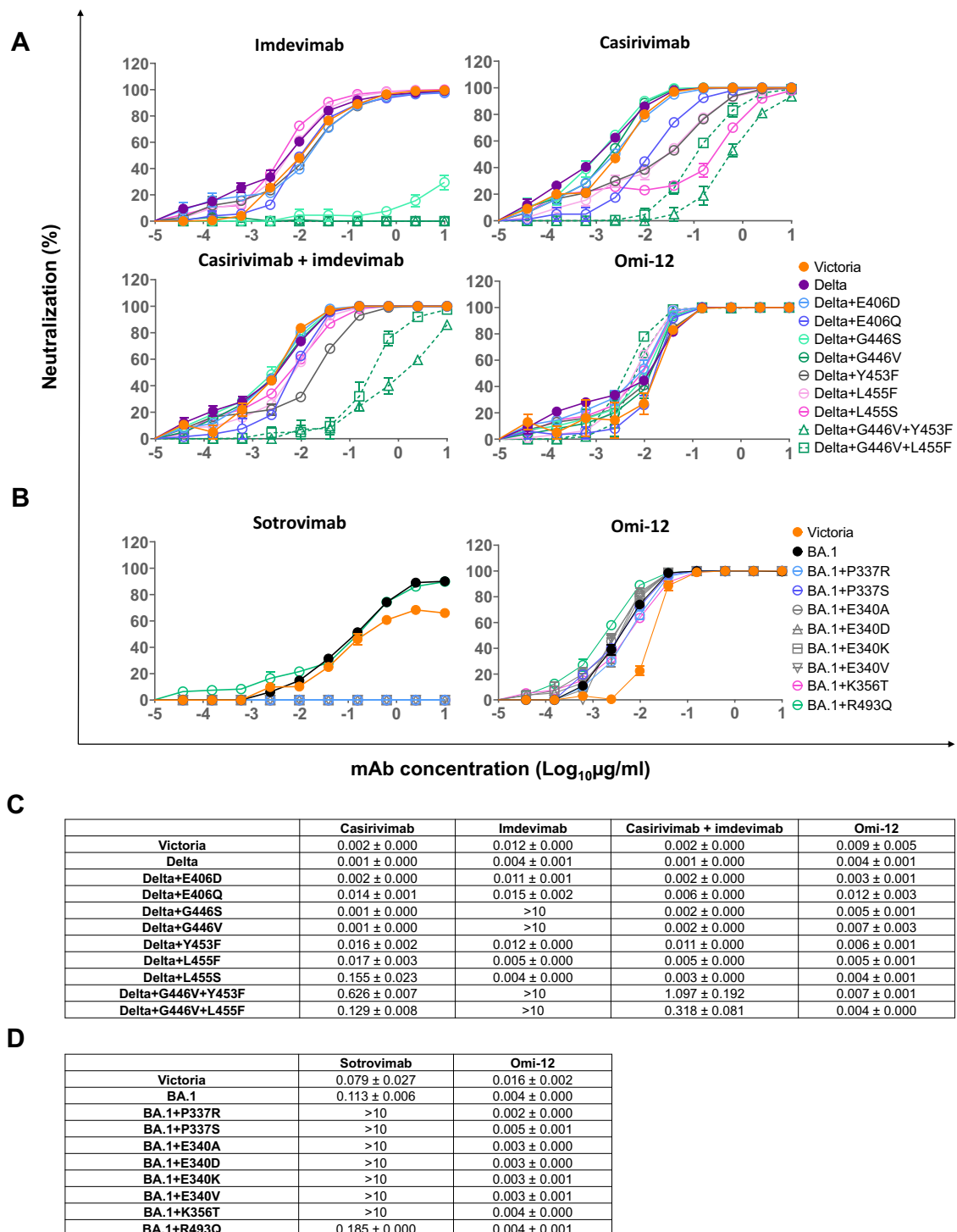
Fig. 3 | Neutralisation escape caused by RBD mutations. A Pseudoviral neutralisation curves of the indicated Delta variants with REGEN-COV mAbs. Comparison is made with Omi-12 A VH1-58 mAb, which is not sensitive to the mutations found following REGEN-COV treatment. Data are presented as mean values ± SEM. $n = 2$ biologically independent experiments. **B** Pseudovirus neutralisation curves for BA.1 sotrovimab mutants. Data are presented as mean values ± SEM. $n = 2$ biologically independent experiments. **C, D** Neutralisation mean IC50 ± SEM titres for neutralisations shown in **A**, **B**.

study did not examine T cells which contribute to the host defence and are less impacted by mutation.

In summary, we demonstrate here mutational changes in viruses isolated from patients treated with mAbs. The mutational profiles of patients treated with sotrovimab or REGEN-COV are strikingly different and the mutations map to the binding sites for the mAb on Delta or BA.1 RBD. The corresponding mutations impair the binding of mAbs to spike RBD, resulting in reduced neutralisation titre. Strikingly, for

REGEN-COV, viruses evolve pairs of mutations to escape both components of the antibody cocktail.

Methods
Ethics statement
Surveillance of coronavirus disease 2019 (Covid-19) testing and vaccination is undertaken under Regulation 3 of the Health Service (Control of Patient Information) Regulations 2002 to collect

Table 3 | A, B Summary of binding affinity between RBDs and therapeutic mAbs (A) casirivimab+imdevimab, (B) sotrovimab

A

RBD	Casirivimab K_D(nM)	Casirivimab Fold reduction	Imdevimab K_D(nM)	Imdevimab Fold reduction
Delta RBD WT	0.36	-	9.4	-
Delta RBD + E406D	7.1	20	15	1.6
Delta RBD + E406Q	14	38	8.9	1.1*
Delta RBD + G4465	0.56	1.6	734	78
Delta RBD + G446V	0.64	1.8	Very weak binding	Very weak binding
Delta RBD + Y453F	67	186	9.8	1.0
Delta RBD + L455F	44	122	11	1.2
Delta RBD + L4555	133	369	9.1	1.0
Delta RBD + G446V + Y453F	125	347	Very weak binding	Very weak binding
Delta RBD + G446V + L455F	69	192	Very weak binding	Very weak binding

B

RBD	Sotrovimab K_D(nM)	Sotrovimab Fold reduction
BA.1 RBD WT	0.17	-
BA. 1 RBD + P337R	753	4428
BA. 1 RBD + P337S	332	1951
BA. 1 RBD + E340A	3415	20088
BA. 1 RBD + E340D	764	4494
BA. 1 RBD + E34OK	3441	20241
BA. 1 RBD + E34OV	345	2027

The fold reduction in affinity between RBD mutants and wild-type RBD is calculated. The number labelled with a star indicates a fold increase in affinity. See also Figs. S2 and 3.

confidential patient information (www.legislation.gov.uk/uksi/2002/1438/regulation/3/made. opens in new tab) under Sections 3(i)(a–c), 3(i)(d) (i) and (ii), and 3. The genomic surveillance study protocol (https://www.gov.uk/government/publications/covid-19-genomic-surveillance-of-patients-who-are-treated-with-neutralising-monoclonal-antibody-or-immunosuppressed) was subject to an internal review by the UKHSA England Research Ethics and Governance Group and was found to be fully compliant with all regulatory requirements. Given that no regulatory issues were identified, and that an ethics review is not a requirement for this type of work, it was decided that a full ethics review, would not be necessary. We did not obtain informed consent nor provide any participant compensation.

Study population

In April 2020, the UK established a national programme of SARS-CoV-2 genomic surveillance through which viruses from a random sample of population positives in the community and hospital have been routinely sequenced[34]. In addition, a protocol was introduced to enhance sequencing coverage of those receiving treatment in hospitals and within the community (including pre-treatment and follow-up sampling). Patients on treatment were linked to their genetic sequences through their COG-IDs. The present analysis includes all patients who have received treatment in the UK, for whom at least one sample had been collected by 12 April 2022 and for whom a viral genetic sequence was available. Because post-treatment datasets were already small, and because we did not expect differences by sex in viral evolution, we did not consider sex or gender in our study design, and did not further link patient information to obtain age, sex or gender.

At this date, the five therapeutic interventions deployed across the population included casirivimab/imdevimab, sotrovimab, molnupiravir, remdesivir and paxlovid (nirmatrelvir plus ritonavir). For each patient, data available include: date of sample, therapeutic intervention/ treatment and date of treatment.

Sequence datasets

The pipeline used to collect and process raw SARS-CoV-2 sequence data and sample-associated metadata across the UK genomic surveillance network has been previously described[35]. A network of sampling sites (including hospitals and testing centres) produces samples and sample metadata. Most clinical samples were nasal/oropharyngeal swabs, but nasopharyngeal aspirates, bronchoalveolar lavage and sputum samples were also collected. Some sampling sites conducted their own sequencing; otherwise, they were connected to a regional sequencing centre or to the Wellcome Sanger institute. Regional sequencing centres include academic institutions, laboratories and public health agencies. The sequences analysed in the present manuscript were all generated through pillar 1, meaning they were collected across the NHS and processed at the sample site or by a university laboratory for a faster turnaround. The sequencing centre extracts and sequences samples. The exact sequencing procedure varied across sites, however, the majority of sites adhered to the ARTIC protocol (https://www.protocols.io/view/ncov-2019-sequencing-protocol-v3-locost-bp2l6n26rgqe/v3), using either Illumina or the Oxford Nanopore Technologies platform. The ARTIC bioinformatics pipeline (https://github.com/connor-lab/ncov2019-artic-nf) then turns SARS-CoV-2 sequencing data into consensus sequences and an alignment of sequence read fragments aligned to the SARS-CoV-2 reference genome (NCBI NC_045512.2). COVID lineages were assigned using Pango v1.3[36].

Analysis of pre- and post-treatment sequences

All sequences from patients known to have undergone treatment were downloaded from CLIMB. Genome alignments were split into gene regions (*spike, nsp5, nsp7, nsp8, nsp9, nsp10, nsp12, nsp14*) and translated to amino acids for analysis. Analyses were conducted for each treatment on the proteins they are theorised to interact with. Analyses were split by variant (Delta, Omicron BA.1 and Omicron BA.2), with
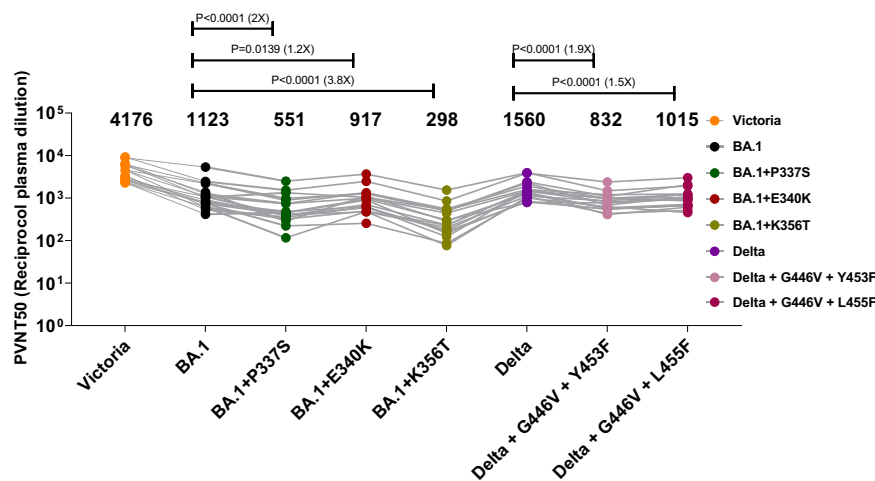
Fig. 4 | Pseudoviral neutralisation IC50 titres of third dose Pfizer-BioNTech vaccine serum. IC50 reciprocal plasma dilution titres for Delta REGEN-COV induced mutations and BA.1 sotrovimab induced mutations are compared with titres for ancestral strain Victoria, Delta and BA.1. Geometric mean of titres are shown above each column. The Wilcoxon matched-pairs signed rank test was used for the analysis and two-tailed P values were calculated. Different colours indicate different pseudovirus, which is indicated underneath the graph.

Delta sublineages (B.1617.2 and all AY lineages) all classified as Delta. As such, each analysis was conducted independently on every treatment, variant and gene region combination of interest (Table S1).

Pre-treatment sequences are those obtained from patients with a sequenced sample within one week prior to treatment initiation (including the day of treatment initiation). The analysis was repeated with a range of cut-offs for defining post-treatment sequences, including post-treatment sequences only if they were sampled at least 1, 5, 10, or 14 days after treatment. Our main analysis uses the 10-day cutoff, and 1, 5 and 14 days are presented as a sensitivity analysis. For each analysis, we split the dataset into pre-and post-treatment sequences. At each site in the alignment, the amino acid frequency was calculated in pre- vs post-treatment sequences, and Fisher's exact test was used to determine whether this probability distribution diverged from the null expectation. In this way, sites that display unexpected differences in amino acid frequencies were identified, and the specific amino acid changes highlighted. Analyses were conducted at the patient-level rather than at the sequence level, so that if a patient had multiple pre- or post-treatment sequences a single sequence was retained, with sequences diverging from the wild-type favoured.

Analysis of UK genomic database
All Delta ($n = 763,511$), BA.1 ($n = 742,992$) and BA.2 ($n = 407,161$) sequences from September 2021 onwards were downloaded from CLIMB, translated to amino acids and split into proteins using an in-house script. For each amino acid site identified in our analysis, amino acid frequencies were tabulated and calculated as proportions of the total number of sequences with a readable amino acid.

Structural modelling/mapping of drug interaction sites
Structural models of RBD-mAbs complexes were generated by super-position of 7ORB [https://www.rcsb.org/structure/7ORB] (RBD with L452R) and Omicron RBD (7TLY [https://www.rcsb.org/structure/7TLY]) with complexes of RBD-casirivimab/imdevimab (6XDG [https://www.rcsb.org/structure/6XDG]) and RBD-sotrovimab (7BEP [https://www.rcsb.org/structure/7BEP]) respectively, using programme SHP[37] to align the RBD domains. Models of 7ORB [https://www.rcsb.org/structure/7ORB] RBD docked with casirivimab/

imdevimab and Omicron RBD docked with sotrovimab were extracted and analysed at drug interaction sites using Coot[38]. Molecular graphics images were generated using UCSF ChimeraX[39].

Sera from Pfizer vaccinees
Pfizer vaccine serum was obtained from volunteers who had received three doses of the BNT162b2 vaccine (Pfizer/BioNTech). Vaccinees were Health Care Workers, based at Oxford University Hospitals NHS Foundation Trust, not known to have prior infection with SARS-CoV-2 and were enrolled in the OPTIC Study as part of the Oxford Translational Gastrointestinal Unit GI Biobank Study 16/YH/0247 [research ethics committee (REC) at Yorkshire & The Humber – Sheffield] which has been amended for this purpose on 8 June 2020. The study was conducted according to the principles of the Declaration of Helsinki (2008) and the International Conference on Harmonisation (ICH) Good Clinical Practice (GCP) guidelines. Written informed consent was obtained for all participants enrolled in the study. Participants were sampled approximately 28 days (median 31, range 28–56), after receiving a third booster dose of Pfizer/BioNtech BNT162b2 mRNA Vaccine, 30 micrograms, administered intramuscularly after dilution (0.3 mL each), 17–28 days apart for dose 1 and 2, then ~9 months apart (range 253–300) for dose 2 and 3. The mean age of vaccinees was 42 years (range 30–59), 10 male and 9 female.

Plasmid construction and pseudotyped lentiviral particles production
Pseudotyped lentivirus expressing SARS-CoV-2 spike proteins for ancestral strains (Victoria, Delta and BA.1) were constructed as described before[29,40] with some modifications. A similar strategy was applied for all variant constructs. Delta and BA.1 were used as the template and the constructs were cloned by PCR amplification of vector and inserts, followed by Gibson assembly. To generate the insert fragments, the overlapping primers for all individual variants were used separately to amplify, together with two primers of pcDNA3.1 vector (pcDNA3.1_BamHI_F and pcDNA3.1_Tag_S_EcoRI_R). The pcDNA3.1 vector was also amplified using

pcDNA3.1_Tag_S_EcoRI_F and pcDNA3.1_BamHI_R primers. The primer pairs used in this study are shown in supplementary (Table S2). All constructs were verified by Sanger sequencing after plasmid isolation using QIAGEN Miniprep kit (QIAGEN). The resulting spike gene-carrying pcDNA3.1 was used for generating pseudoviral particles together with the lentiviral packaging vector and transfer vector encoding luciferase reporter.

Pseudoviral neutralisation assay
The details of the pseudoviral neutralisation test were described previously[19,40] with some modifications. Briefly, a fourfold serial dilution of each mAb, starting from 10 μg/ml, was incubated with pseudoviral particles at 37 °C, 5% CO_2 for 1 h. The stable HEK293T/17 cells (ATCC, CRL-11268) expressing human ACE2 were then added to the mixture at 1.5×10^4 cells/well. At 48 h post transduction, culture supernatants were removed and 50 μL of 1:2 Bright-GloTM Luciferase assay system (Promega, USA) in 1× PBS was added into each well. The reaction was incubated at room temperature for 5 min and the firefly luciferase activity was measured using CLARIOstar (BMG Labtech, Ortenberg, Germany). The percentage of neutralisation was calculated relative to the control. Probit analysis was used to estimate the value of dilution that inhibits half of the maximum pseudotyped lentivirus infection (PVNT50). Antibodies included in the study were Imdevimab (Regeneron), Casirivimab (Regeneron) and Sotrovimab (GSK). To determine the neutralising activity of vaccine sera, 3-fold serial dilutions starting from neat samples were incubated with pseudoviral particles for 1 hr and the same strategy as mAb was applied. The primer sequences used to generate pseudoviruses are listed in Table S2.

Cloning of RBDs
To generate the His-tagged construct of RBDs, site-directed PCR mutagenesis was performed using the Delta or BA.1 pseudovirus plasmid construct as the template, or pseudovirus plasmid construct containing the desired RBD mutant was used as the template for amplification of the RBD gene fragment.

The template, primers and expression vectors used for cloning of each RBD are shown in Table S3 and the primer sequences are shown in Table S4.

Cloning was performed using the ClonExpress II One Step Cloning Kit (Vazyme). The Constructs were verified by Sanger sequencing after plasmid isolation using QIAGEN Miniprep kit (QIAGEN).

Production of RBDs
Plasmids encoding RBDs were transfected into Expi293F™ Cells (Gibco, A14527) by PEI, cultured in FreeStyle™ 293 Expression Medium (ThermoFisher) at 30 °C with 8% CO_2 for 3 days. The conditioned medium was diluted 1:2 into binding buffer (50 mM sodium phosphate, 500 mM sodium chloride, pH 8.0). RBDs were purified with a 5 mL HisTrap nickel column (GE Healthcare) through His-tag binding, followed by a Superdex 75 10/300 GL gel filtration column (GE Healthcare) in 10 mM HEPES and 150 mM sodium chloride.

Surface plasmon resonance
The surface plasmon resonance experiments were performed using a Biacore T200 (GE Healthcare). All assays were performed with a running buffer of HBS-EP (Cytiva) at 25 °C. A Protein A sensor chip (Cytiva) was used. The mAb as indicated was immobilised onto the sample flow cell of the sensor chip. The reference flow cell was left blank.

To determine the binding kinetics, RBD was injected over the two flow cells at a range of five concentrations prepared by serial twofold dilutions, at a flow rate of 30 μl min⁻¹ using a single-cycle kinetics programme. Running buffer was also injected using the same programme for background subtraction. All data were fitted to a 1:1

binding model using Biacore T200 Evaluation Software 3.1. To determine the binding affinity (where kinetics were difficult to determine), RBD was injected over the two flow cells at a range of concentrations prepared by serial two-fold dilutions, at a flow rate of 30 μl min⁻¹. Running buffer was also injected using the same programme for background subtraction. All KD data were fitted to a 1:1 binding model using Biacore T200 Evaluation Software 3.1; the figures were plotted with GraphPad Prism 9.

To compare the binding profiles between Delta RBD + G446V / Delta RBD + G446V + Y453F/Delta RBD + G446V + L455F and Delta RBD WT for imdevimab, a single injection of RBD was performed over the two flow cells at 1 μM, at a flow rate of 30 μl min⁻¹. Running buffer was also injected using the same programme for background subtraction. The sensorgrams were plotted using Prism9 (GraphPad).

Reporting Summary
Further information on research design is available in the Nature Portfolio Reporting Summary linked to this article.

Data availability
Reagents generated in this study are available from David Stuart with a completed Materials Transfer Agreement. The SARS-CoV-2 genomic data generated in this study have been deposited in Genbank. The list of IDs are provided in Supplementary Data 1. Source Data for all figures are provided as a Source Data file. Information on clinical treatments at the individual level, linked to sequence ID are under restricted access for patient confidentiality reasons, but access can be obtained by individuals upon submission of a reasonable research proposal sent to Meera Chand Meera.Chand@ukhsa.gov.uk and signing of a data sharing agreement.

Code availability
Analysis was performed through a series of scripts available on github (https://github.com/manonr/covid-therapeutics). A permanent link to version of the code used in this study is available at https://github.com/manonr/covid-therapeutics/releases/tag/v.1.0-2023-01.

References
1. Zhou, P. et al. A pneumonia outbreak associated with a new coronavirus of probable bat origin. *Nature* **579**, 270–273 (2020).
2. Obermeyer, F. et al. Analysis of 6.4 million SARS-CoV-2 genomes identifies mutations associated with fitness. *Science* **376**, 1327–1332 (2022).
3. Supasa, P. et al. Reduced neutralization of SARS-CoV-2 B.1.1.7 variant by convalescent and vaccine sera. *Cell* **184**, 2201–2211.e2207 (2021).
4. Micochova, P. et al. SARS-CoV-2 B.1.617.2 delta variant replication and immune evasion. *Nature* **599**, 114–119 (2021).
5. Dejnirattisai, W. et al. SARS-CoV-2 omicron-B.1.1.529 leads to widespread escape from neutralizing antibody responses. *Cell* **185**, 467–484.e415 (2022).
6. Zhou, D. et al. Evidence of escape of SARS-CoV-2 variant B.1.351 from natural and vaccine-induced sera. *Cell* **184**, 2348–2361.e2346 (2021).
7. Dejnirattisai, W. et al. Antibody evasion by the P.1 strain of SARS-CoV-2. *Cell* **184**, 2939–2954.e2939 (2021).
8. Dejnirattisai, W. et al. The antigenic anatomy of SARS-CoV-2 receptor binding domain. *Cell* **184**, 2183–2200.e2122 (2021).
9. Yuan, M. et al. Structural basis of a shared antibody response to SARS-CoV-2. *Science* **369**, 1119–1123 (2020).
10. Yuan, M. et al. A highly conserved cryptic epitope in the receptor binding domains of SARS-CoV-2 and SARS-CoV. *Science* **368**, 630–633 (2020).
11. Huo, J. et al. Neutralization of SARS-CoV-2 by destruction of the prefusion spike. *Cell Host Microbe* **28**, 445–454 (2020).

12. Zhou, D. et al. Structural basis for the neutralization of SARS-CoV-2 by an antibody from a convalescent patient. *Nat. Struct. Mol. Biol.* **27**, 950–958 (2020).

13. Feder, A. F., Harper, K. N., Brumme, C. J. & Pennings, P. S. Understanding patterns of HIV multi-drug resistance through models of temporal and spatial drug heterogeneity. Elife **10**, https://doi.org/10.7554/eLife.69032 (2021).

14. Arts, E. J. & Hazuda, D. J. HIV-1 antiretroviral drug therapy. *Cold Spring Harb. Perspect. Med.* **2**, a007161 (2012).

15. Diallo, D. et al. Antituberculosis therapy and gut microbiota: review of potential host microbiota directed-therapies. *Front. Cell Infect. Microbiol.* **11**, 673100 (2021).

16. Hansen, J. et al. Studies in humanized mice and convalescent humans yield a SARS-CoV-2 antibody cocktail. *Science* **369**, 1010–1014 (2020).

17. Al-Obaidi, M. M. et al. Effectiveness of casirivimab-imdevimab monoclonal antibody treatment among high-risk patients With severe acute respiratory syndrome coronavirus 2 B.1.617.2 (Delta Variant) infection. *Open Forum Infect. Dis.* **9**, ofac186 (2022).

18. Baum, A. et al. Antibody cocktail to SARS-CoV-2 spike protein prevents rapid mutational escape seen with individual antibodies. *Science* **369**, 1014–1018 (2020).

19. Liu, C. et al. Reduced neutralization of SARS-CoV-2 B.1.617 by vaccine and convalescent serum. *Cell* **184**, 4220–4236.e4213 (2021).

20. Copin, R. et al. The monoclonal antibody combination REGEN-COV protects against SARS-CoV-2 mutational escape in preclinical and human studies. *Cell* **184**, 3949–3961.e3911 (2021).

21. Pinto, D. et al. Cross-neutralization of SARS-CoV-2 by a human monoclonal SARS-CoV antibody. *Nature* **583**, 290–295 (2020).

22. McCallum, M. et al. Structural basis of SARS-CoV-2 Omicron immune evasion and receptor engagement. *Science* **375**, 864–868 (2022).

23. Di Genova, C. et al. Production, titration, neutralisation and storage of SARS-CoV-2 lentiviral pseudotypes. *figshare*, https://doi.org/10.6084/m9.figshare.13502580.v2 (2020).

24. Cele, S. et al. Omicron extensively but incompletely escapes Pfizer BNT162b2 neutralization. *Nature*, https://doi.org/10.1038/s41586-021-04387-1 (2021).

25. Wolter, N. et al. Early assessment of the clinical severity of the SARS-CoV-2 omicron variant in South Africa: a data linkage study. *Lancet* **399**, 437–446 (2022).

26. Weinreich, D. M. et al. REGEN-COV antibody combination and outcomes in outpatients with Covid-19. *N. Engl. J. Med.* **385**, e81 (2021).

27. Gupta, A. et al. Early treatment for Covid-19 with SARS-CoV-2 neutralizing antibody sotrovimab. *N. Engl. J. Med.* **385**, 1941–1950 (2021).

28. Mahase, E. Covid-19: has the spread of omicron BA.2 made antibody treatmnets redundant? *BMJ* **377**, o1009 (2022).

29. Nutalai, R. et al. Potent cross-reactive antibodies following Omicron breakthrough in vaccinees. *Cell* **185**, 2116–2131.e2118 (2022).

30. Rockett, R. et al. Resistance mutations in SARS-CoV-2 delta variant after sotrovimab use. *N. Engl. J. Med.* **386**, 1477–1479 (2022).

31. Starr, T. N. et al. Prospective mapping of viral mutations that escape antibodies used to treat COVID-19. *Science* **371**, 850–854 (2021).

32. Choi, B. et al. Persistence and evolution of SARS-CoV-2 in an immunocompromised host. *N. Engl. J. Med.* **383**, 2291–2293 (2020).

33. Greninger, A. L. et al. Clinical and infection prevention applications of severe acute respiratory syndrome coronavirus 2 genotyping: an Infectious Diseases Society of America/American Society for Microbiology Consensus Review Document. *J. Clin. Microbiol* **60**, e0165921 (2022).

34. The COVID-19 Genomics UK (COG-UK) consortium. An integrated national scale SARS-CoV-2 genomic surveillance network. *Lancet Microbe* **1**, e99–e100 (2020).

35. Nicholls, S. M. et al. CLIMB-COVID: continuous integration supporting decentralised sequencing for SARS-CoV-2 genomic surveillance. *Genome Biol.* **22**, 196 (2021).

36. O'Toole, A., Pybus, O. G., Abram, M. E., Kelly, E. J. & Rambaut, A. Pango lineage designation and assignment using SARS-CoV-2 spike gene nucleotide sequences. *BMC Genomics* **23**, 121 (2022).

37. Stuart, D. I., Levine, M., Muirhead, H. & Stammers, D. K. Crystal structure of cat muscle pyruvate kinase at a resolution of 2.6 A. *J. Mol. Biol.* **134**, 109–142 (1979).

38. Casanal, A., Lohkamp, B. & Emsley, P. Current developments in Coot for macromolecular model building of electron cryo-microscopy and crystallographic data. *Protein Sci.* **29**, 1069–1078 (2020).

39. Pettersen, E. F. et al. UCSF ChimeraX: structure visualization for researchers, educators, and developers. *Protein Sci.* **30**, 70–82 (2021).

40. Nie, J. et al. Establishment and validation of a pseudovirus neutralization assay for SARS-CoV-2. *Emerg. Microbes Infect.* **9**, 680–686 (2020).

Acknowledgements

Author contributions

M.R.C., S.R., G.R.S. and D.I.S. conceived of the study. M.R.C. performed the post-treatment analyses. N.G. performed the UK genomic surveillance analyses. R.N., A.D.-G., R.D., A.T., P.S., C.L., M.S., D.Z. and J.H. performed experiments, J.H., J.M., M.C. designed experiments, P.K. and S.J.D. oversaw the OPTIC study for the collection of vaccine serum, as part of the PITCH consortium. M.B., J.R., E.F. and D.I.S. performed structure analyses. N.G., H.H., N.E., M.S., C.B., S.H. and S.R. analysed sequence data. M.R.C., G.R.S., J.H. and D.I.S. wrote the first draft of the manuscript. All authors reviewed and approved the final manuscript.

Competing interests

Additional information